Numerical accuracy of magnetotelluric modeling: A comparison of finite difference approximations

Weerachai Siripunvaraporn[1], Gary Egbert[2], and Yongwimon Lenbury[3]

[1]*Department of Physics, Faculty of Science, Mahidol University, Rama VI Rd., Rachatawee, Bangkok, 10400, Thailand*
[2]*College of Oceanic and Atmospheric Sciences, Oregon State University, Corvallis, OR 97331, U.S.A.*
[3]*Department of Mathematics, Faculty of Science, Mahidol University, Rama VI Rd., Rachatawee, Bangkok, 10400, Thailand*

To solve for the induced electromagnetic fields in a conductive medium the quasi-static Maxwell's equations may be reduced to a second order elliptic system, formulated in terms of either the electric or magnetic vector fields. We show with 1-D and 3-D numerical experiments that solutions obtained from equations formulated in terms of the electric fields are less sensitive to grid resolution than those obtained from the magnetic formulation. On a fine enough mesh, solutions from both approaches are nearly identical, while on coarser meshes solutions form the electric field formulation tend to be closer to exact solutions (where available), or fully converged fine mesh solutions.

1. Introduction

For complicated and geologically realistic 3-D models, numerical approaches based on the finite difference method (e.g., Mackie *et al.*, 1994; Smith, 1996b) or the finite element method (e.g., Wannamaker *et al.*, 1987), are generally more efficient and robust for computing electromagnetic (EM) responses than the integral equation technique (e.g., Wannamaker, 1991). To obtain magnetotelluric (MT) responses at the surface, one must solve for the electric (**E**) and magnetic (**H**) fields simultaneously via the first order Maxwell's equations,

$$\nabla \times \mathbf{H} = \sigma \mathbf{E}, \qquad (1)$$

$$\nabla \times \mathbf{E} = i\omega\mu\mathbf{H}, \qquad (2)$$

subject to appropriate boundary conditions at the top, bottom and sides of the domain. Here μ is the air magnetic permeability, ω is the angular frequency, and σ is the conductivity (the inverse of resistivity, ρ). The same equations, with addition of source terms (and different boundary conditions), must be solved for more general EM modeling problems.

Solving the coupled system (1) and (2) requires substantial computer memory (Mackie *et al.*, 1994). Memory requirements can be significantly reduced by solving the second order Maxwell's equations, in **E** form,

$$\nabla \times \nabla \times \mathbf{E} = i\,\omega\mu\sigma\mathbf{E}, \qquad (3)$$

or, in **H** form,

$$\nabla \times \rho \nabla \times \mathbf{H} = i\,\omega\mu\mathbf{H}. \qquad (4)$$

The boundary condition for (3) and (4) are specified tangential fields on the edges of the model domain. For the MT

problem, fields at the top of the domain (in the air) are a given constant, while those at the bottom are generally assigned from 1-D calculations, and those for the sides come from a 2-D calculation. The secondary fields (i.e., **H** when (3) is solved, or **E** when (4) is solved) are then computed directly from the first order Maxwell's equations. This approach has proven to be computational efficient and reliable, and forms the basis for most modern 3-D modeling codes. Mackie *et al.* (1994) developed a staggered grid finite difference (SFD) scheme to solve (4), while Smith (1996b) applied a similar technique to (3). The algorithms consist of solving the linear system of equations, obtained by discretizing (3) or (4), via iterative relaxation methods. Preconditioners and a "divergence correction" are used to accelerate the convergence rate, and correct for the nonzero divergence of the solutions (Mackie *et al.*, 1994; Smith, 1996b).

There are two ways to define the numerical grid for the SFD approximation. Both Mackie *et al.* (1994) and Smith (1996a, b) specify **E** at the middle faces of the blocks, and **H** at the center along the block's edges (Fig. 1(a)). Alternatively, one can specify **E** along the block edges and **H** on the block faces (Fig. 1(b)). This formulation has been used by Yee (1966), Wang and Hohmann (1993) and Newman and Alumbaugh (1997). With σ (or ρ) defined for each block, the grid convention of Fig. 1(a) would appear to be more natural, since continuity of electric current $\mathbf{J} = \sigma\mathbf{E}$ across faces is then readily enforced. However, the boundary conditions are specified more naturally for **E** when the EM fields are discretized as in Fig. 1(b), so the best choice of grid convention is not obvious. Ignoring differences in numerical implementation of boundary conditions, it is readily verified that the discrete system for **E** and **H** given by (3) and (2) is algebraically equivalent to that given by (4) and (1), provided a consistent grid is used. Difference between these two solution approaches on a consistent grid can still arise due
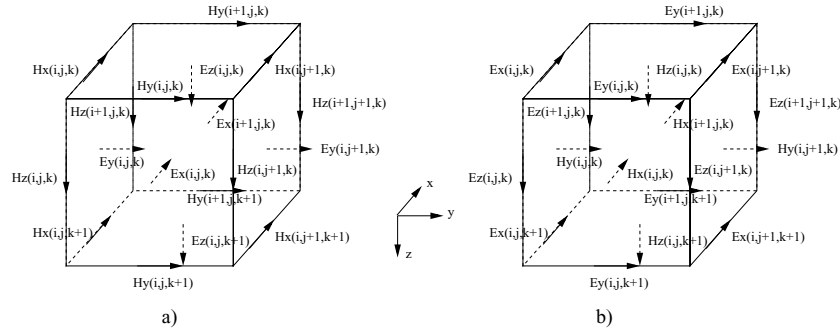
Fig. 1. Three-dimensional finite difference grids. a) In solving (4) for **H**, the magnetic fields are sampled at the centers of the edges of each cube, and the electric fields at the centers of the faces. b) In solving (3) for **E**, the electric fields are sampled at the centers of the edges of each cube, and the magnetic fields at the centers of the faces.
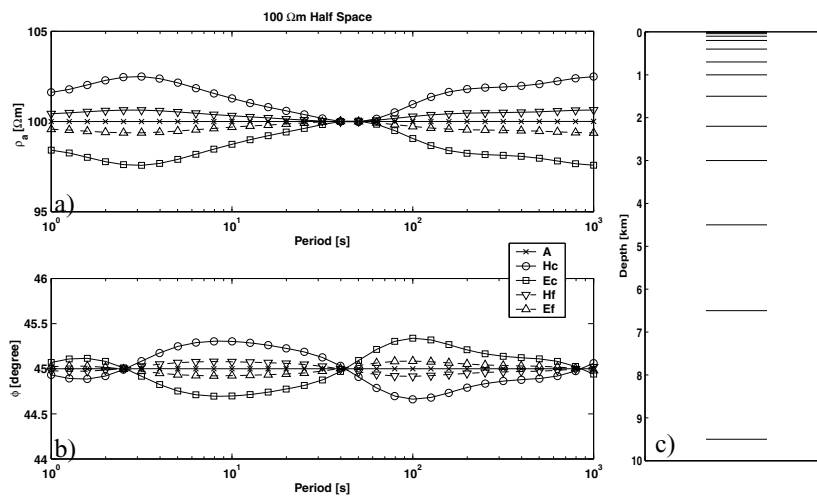

Fig. 2. Apparent resistivities (a) and phases (b) as a function of period, for the 100 Ω-m half space model. The upper 10 km of the coarse grid discretization (with total of 26 nodes) is shown in (c). The node spacing is cut by half for a total of 52 nodes for higher grid resolution. A: Solutions obtained from analytical formulation, Hc: Solutions obtained from FDH with coarse grid resolution, Ec: Solutions obtained from FDE with coarse grid resolution, Hf: Solutions obtained from FDH with fine grid resolution, Ef: Solutions obtained from FDE with fine grid resolution.

to specification of boundary condition, and numerical round off.

We have developed algorithms based on the SFD grid approximations to solve for either **E** via (3) with the grid convention of Fig. 1(b) (referred to as FDE) or **H** via (4) with the grid in Fig. 1(a) (referred to as FDH) on a standard desktop PC. The difference between our codes and the program by Mackie *et al.* (1994) and Smith (1996b) is that the linear system of equations for FDE and FDH are solved via the quasi-minimum residual (QMR) method. Mackie *et al.* (1994) used the minimum residual method, and Smith (1996b) preferred the biconjugate gradient method. Also for FDE we define our grid convention as in Fig. 1(b), where Smith (1996a, b) followed the convention of Fig. 1(a). The preconditioner is similar to that of Mackie *et al.* (1994), but with an incomplete LU decomposition replacing the Cholesky decomposition. The secondary fields required to compute MT responses are extrapolated to the surface using (1) and (2) as in Mackie *et al.* (1994). A divergence correction, very similar to that of Mackie *et al.* (1994) or Smith (1996b), was also applied in FDE and FDH, to ensure divergence free currents and magnetic fields, respectively.

Accuracy of the solution depends on three factors: the grid

resolution, the numerical scheme used to define the coefficient matrix (e.g., the different conventions of Fig. 1), and the numerical accuracy of the linear equation solver. A finer mesh generally yields higher accuracy, but at the cost of long computing times and larger memory requirements. Thus, mesh resolution is limited in practice by the computational resources. In this paper, we consider the differences between the two solution approaches (FDE and FDH) and their dependence on grid resolution.

2. Numerical Examples

Figure 2 displays apparent resistivities and phases computed with FDE and FDH for a 100 Ω-m half space model. Two different mesh resolutions are used, each with nearly logarithmic spacing in the vertical. The first upper 10 km of the coarse mesh is shown in Fig. 2(c); node spacing is reduced by a factor of two for the fine mesh. Since the model is exactly 1-D, the horizontal grid discretization should have no effect on solutions. After verifying that this is the case, further numerical analysis for this simple case was based on 1-D codes. With nearly logarithmic vertical mesh spacing and a homogeneous (half space) model, the discretization errors from both FDE and FDH do not vary significantly with
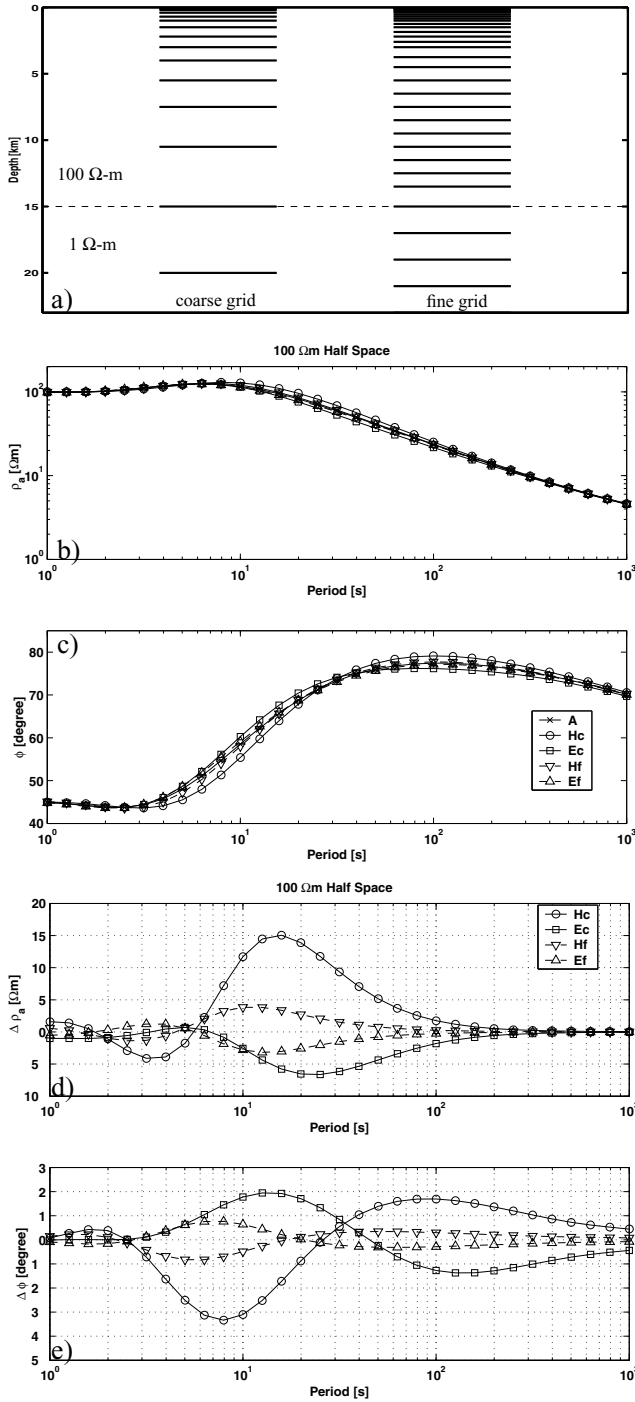
Fig. 3. (a) The 2-D layered Earth model with two grid discretizations. Apparent resistivities (b) and phases (c) as a function of period, and (d)–(e) their respective errors, for solutions labeled as in Fig. 2.

Table 1. The overall deviations from the analytical solutions of the solutions obtained in Fig. 3.

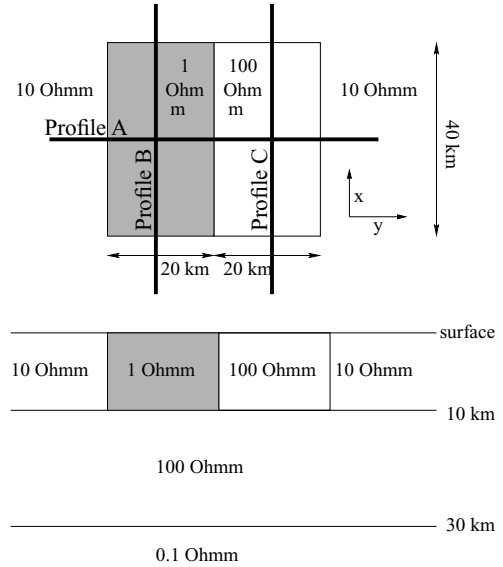|	ρ_a	ϕ
ε_{Hc}	1.167	0.285
ε_{Ec}	0.547	0.181
ε_{Hf}	0.264	0.062
ε_{Ef}	0.245	0.059

Fig. 4. Plan view (upper panel) of the 3-D model (Mackie *et al.*, 1993) with conductive (1 Ω-m) and resistive (100 Ω-m) prisms buried in a layered Earth (lower panel).

period. Other mesh designs will behave somewhat differently.

The overall deviation of the solution (x_i) from the reference solution (x_i^r) is given as

$$\varepsilon = \frac{1}{N}\sqrt{\sum_i^N (x_i - x_i^r)^2}, \quad (5)$$

where, N is the total number of data. In this calculation, the reference is the 1-D analytical solution. For a fixed mesh, de-

viations in solutions obtained from the two approaches vary consistently, but in the opposite sense with under estimation at some periods and over estimation at other periods. The overall deviation of both algorithms relative to the analytical solutions for the coarse mesh are very small and almost identical at 0.300 Ω-m for apparent resistivity and 0.035 degrees for phase. Deviations are reduced by a factor of roughly 4 to 0.078 Ω-m for apparent resistivity and 0.009 degrees for phase on a finer mesh. This very simple numerical experiment shows us that on a homogeneous structure the deviation levels for both algorithms are similar, and are roughly quadratic in grid resolution, as would be expected for the centered difference approximation of the staggered grid (e.g., Press *et al.*, 1992).

2.1 1-D layered Earth

Next, we applied both algorithms to 1-D layered Earth models. Figure 3 shows the apparent resistivities and phases, and their deviations for a model consisting of a 100 Ω-m 15 km thick layer over a 1 Ω-m basement. The model is vertically discretized at two resolutions: a coarse mesh (Fig. 3(a) left) with total of 26 nodes and a refined mesh (Fig. 3(a) right) with total of 55 nodes, and higher resolution particularly near the resistivity contrast. Again the model is exactly 1-D so tests were conducted using 1-D codes. Table 1 displays the overall deviation values computed with equation (5) for the solutions of Fig. 3 relative to the analytical solu-
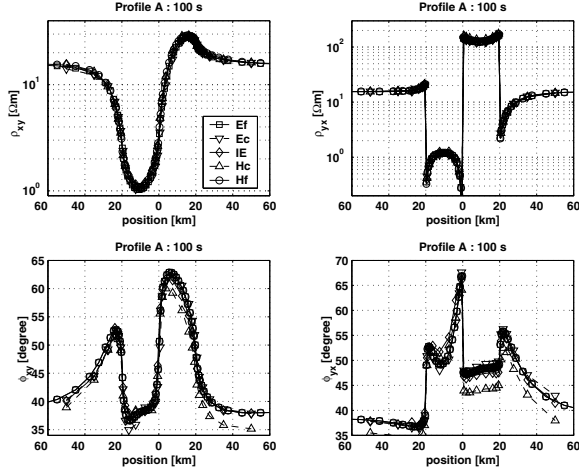
Fig. 5.   Apparent resistivities (top row) and phases (bottom row) across profile A at 100 s for H_y polarization (left panel) and H_x polarization (right panel). Ef: responses obtained from solving **E** using fine mesh, Ec: responses obtained from solving **E** using coarse mesh, Hc: responses obtained from solving **H** using coarse mesh, Hf: responses obtained from solving **H** using fine mesh, IE: responses obtained from using the integral equation approach (Wannamaker, 1991).
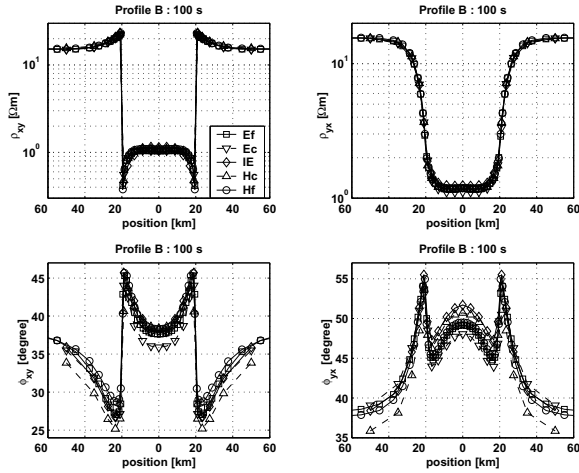

Fig. 7.   Apparent resistivities (top row) and phases (bottom row) across profile C at 100 s for H_y polarization (left panel) and H_x polarization (right panel). Solutions are labeled as in Fig. 5.

Fig. 6.   Apparent resistivities (top row) and phases (bottom row) across profile B at 100 s for H_y polarization (left panel) and H_x polarization (right panel). Solutions are labeled as in Fig. 5.

Fig. 8.   Plots of deviations calculated from (5) between coarse and fine grid FDE and FDH solutions for profile B (left) and profile C (right). EcHc: Deviation of coarse grid FDE solutions from coarse grid FDH solutions. EfHf: Deviation of fine grid FDE solutions from fine grid FDH solutions. EcEf: Deviation of coarse grid FDE solutions from fine grid FDE solutions. HcHf: Deviation of coarse grid FDH solutions from fine grid FDH solutions.

tion.

Figure 3(d) and (e) and Table 1 show that at most periods the fine mesh generates significantly smaller deviations (ε_{Hf} and ε_{Ef}) that are generally of similar magnitude for both FDE and FDH, as in the half space case. However, for the coarse mesh, deviation levels for the two algorithms (ε_{Hc} and ε_{Ec}) are significantly smaller for FDE than for FDH. For short periods, discrepancies from the analytical solutions are small and nearly the same for both solutions. However, as the period increases and fields penetrate the conductive basement (over the transition range 2–200 s) the discrepancies from the analytical solution increase, especially for responses obtained from FDH. At longer periods, the deviations from both FDE and FDH are again smaller and of similar magnitude.

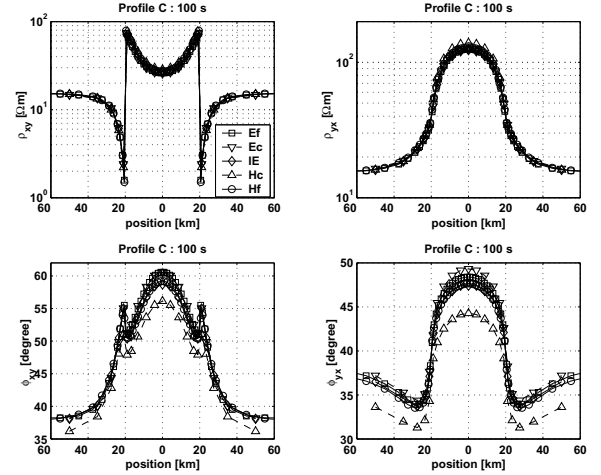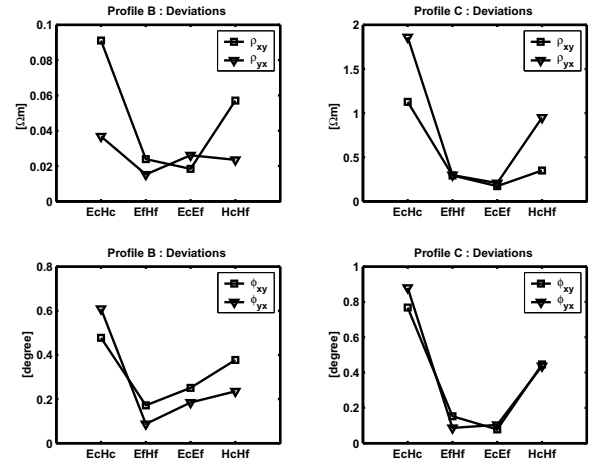The results of Fig. 3 are typical of a larger set of experi-

ments with 1-D Earth models with sharp resistivity gradients, including cases with conductive layers overlying a resistive basement, and models with multiple layers. With a coarse mesh the overall deviation generated from FDE is generally smaller than that from FDH, particularly in the transition periods (as in Fig. 3). With fine enough grid discretization, the solutions from both algorithms are nearly equal to the analytical solution, and errors are of comparable magnitude. These numerical examples on 1-D layered Earth suggests that for coarse grids (due to limited resources or inexperience), FDE can provide better accuracy than FDH.

2.2   3-D structure

To see if the above result holds more generally, we consider differences between numerical solutions obtained from FDE and FDH for a simple, and standard, 3-D case. The model consists of resistive and conductive blocks buried in

a layered Earth (Fig. 4). The responses generated from this model have been previously shown in numerous publications using different modeling techniques, including integral equations (IE; Wannamaker, 1991), and finite difference (Mackie *et al.*, 1993). Two grid discretizations are used for FDE and FDH in our computations. The first grid is discretized as in Mackie *et al.* (1994); 21 blocks in *x*, 28 blocks in *y* and 11 blocks in *z* (with 7 air layers). A second mesh is more finely divided in all directions with 58 blocks in *x*, 74 blocks in *y* and 30 blocks in *z*, with higher resolution near the resistivity contrasts. Resolution of the second mesh was limited by computer resources available in our PC implementation. The finite difference solutions presented in this paper are the final fully converged iterative solutions, with normalized residuals less than 10^{-10}.

In the previous section, we focused on errors as a function of period. Here, we consider the difference of the responses as a function of position on the surface at a fixed period. Figures 5, 6 and 7 display the calculated responses of profiles A, B and C (Fig. 4), respectively, at a period of 100 seconds where the discrepancies are greatest. The responses from both meshes are plotted on the same figure, along with responses computed with the IE technique discretized as in Wannamaker (1991). Most of calculated responses from both FDE and FDH agree very well with the IE solutions (Figs. 5, 6 and 7). However, the reader is reminded that the IE solutions also depend on grid resolution (Wannamaker, 1991; Mackie *et al.*, 1993). Therefore, the IE solutions used here cannot be treated as exact as for the analytical 1-D solutions, but rather only provide reference solutions. Most responses from FDE and FDH agree well with the IE solutions. However, some discrepancies can be clearly observed, particularly in the phase.

In Fig. 8 we plot deviations calculated from (5) between coarse and fine grid FDE and FDH solutions for profiles B and C. Figure 8 shows that the difference between FDE and FDH solutions on a coarse grid (EcHc) are high, but significantly reduced when a finer mesh is used (EfHf). This suggest that the FDE and FDH solutions converge to a common solutions as the grid is refined. The deviations between the solutions produced by FDE with coarse-fine grids (EcEf) are almost always lower than the corresponding deviations from FDH (HcHf). This demonstrate that solutions from FDE are less sensitive to grid resolution than solutions from FDH. Results from other periods and other models with sharp resistivity contrast produce similar results. The reasons for FDE to be less sensitive to the grid resolution than FDH for both 1-D and 3-D cases are unclear at the present.

3. Conclusions

We have developed PC based algorithms based on the staggered grid finite difference approximation to solve the second order Maxwell's equations in both **E** (FDE) and **H** (FDH) forms. With a consistent grid convention, solutions obtained by solving for either **E** or **H** are theoretically identical, if the same boundary condition are applied. However, our algorithms (FDE and FDH) used different grid conventions designed for natural boundary condition specification, i.e., **E** is on the edges for FDE, and **H** is on the edges for FDH. Comparison of solutions from the two algorithms reveal that on a fine enough mesh, both algorithms generate nearly identical solutions, but there are significant differences for a coarse grid discretization. On a coarse grid, FDE generally produces a solution that is closer than FDH to the exact solution (for the 1-D case) and to fully converged fine mesh solutions (for 3-D). We therefore conclude that the solutions obtained from (3), or in **E** form, are likely to be better suited to an inversion algorithm where one fixed grid is used throughout the process, making it hard to define precisely whether the grid used is coarse or fine.

References

Mackie, R. L., T. R. Madden, and P. E. Wannamaker, Three-dimensional magnetotelluric modeling using difference equations: Theory and comparisons to integral equation solutions, *Geophysics*, **58**, 215–226, 1993.

Mackie, R. L., J. T. Smith, and T. R. Madden, Three-dimensional electromagnetic modeling using finite difference equations: The magnetotelluric example, *Radio Science*, **29**, 923–935, 1994.

Newman, G. A. and D. L. Alumbaugh, Three-dimensional massively parallel electromagnetic inversion—I. Theory, *Geophys. J. Int.*, **128**, 345–354, 1997.

Press, W. H., S. A. Teukolsky, W. T. Vetterling, and B. P. Flannery, *Numerical Recipes in FORTRAN: the art of scientific computing: 2nd*, Cambridge University Press, 1992.

Smith, J. T., Conservative modeling of 3-D electromagnetic fields, Part I: Properties and error analysis, *Geophysics*, **61**, 1308–1318, 1996a.

Smith, J. T., Conservative modeling of 3-D electromagnetic fields, Part II: Biconjugate gradient solution and an accelerator, *Geophysics*, **61**, 1319–1324, 1996b.

Wang, T. and G. W. Hohmann, A finite-difference, time-domain solution for three-dimensional electromagnetic modeling, *Geophysics*, **58**, 797–809, 1993.

Wannamaker, P. E., J. A. Stodt, and L. Rijo, A stable finite element solution for two-dimensional magnetotelluric modelling, *Geophys. J. Roy. Astron. Soc.*, **88**, 277–296, 1987.

Wannamaker, P. E., Advances in three-dimensional magnetotelluric modeling using integral equations, *Geophysics*, **56**, 1716–1728, 1991.

Yee, K. S., Numerical solution of initial boundary value problems involving Maxwell's equations in isotropic media, *IEEE. Trans. Anten. Propag.*, **AP-14**, 302–307, 1966.

W. Siripunvaraporn (e-mail: scwsp@mahidol.ac.th), G. Egbert, and Y. Lenbury